Semiconductor Physics, Quantum Electronics & Optoelectronics, 2009. V. 12, N 4. P. 315-320.

PACS 73.20.Mf, 78.67.Bf

Local plasmons contribution into photocurrent of Au/GaAs surface barrier structure with Au nanoparticles on interface

S. Mamykin[1], N. Dmitruk[1], A. Korovin[1], D. Naumenko[1], A. Dmytruk[2], Yeon-Su Park[2,3]
[1]*V. Lashkaryov Institute of Semiconductor Physics, NAS of Ukraine, 41, prospect Nauky, 03028 Kyiv, Ukraine*
[2]*Center for Interdisciplinary Research, Tohoku University, Sendai 9808578, Japan*
[3]*Graduate School Engineering, Nagoya University, Nagoya 4648601, Japan*
Corresponding author e-mail: mamykin@isp.kiev.ua

Abstract. Au/SiO_2 core-shell nanoparticles have been used to increase the photocurrent in the surface barrier structure Au/GaAs. The method for theoretical calculation of interaction between light and the system of ordered nanoparticles placed on the surface barrier structures has been proposed. Local plasmons excited in the nanoparticles produce additional carriers due to scattering, prolonged interaction with semiconductor and enhanced evanescent electromagnetic field, thus they increase the photocurrent.

Keywords: Au nanoparticles, photocurrent enhancement, plasmonic solar cells.

Manuscript received 25.06.09; accepted for publication 10.09.09; published online 30.10.09.

1. Introduction

Local plasmons in metallic nanoparticles (NPs) of different sizes attract significant attention due to wide applications in optoelectronics and sensorics. These modes can be excited within the spectral range from UV to near IR depending on metal used, particle size and shape, as well as their arrangement. The aim of this work is to study the influence of local plasmon excitation (LPE) on the photocurrent in Au/GaAs surface barrier structures.

Metal nanoparticles are strong scatterers of light at wavelengths near the plasmon resonance, which is due to a collective surface oscillation of conduction electrons in metal. For particles with diameters well below the light wavelength, a point dipole model describes the absorption and scattering of light well. The scattering and absorption cross-sections are given by [1]:

$$C_{\text{scat}} \equiv \frac{1}{6\pi}\left(\frac{2\pi}{\lambda}\right)^4 |\alpha|^2, \qquad C_{\text{abs}} = \left(\frac{2\pi}{\lambda}\right)\text{Im}(\alpha), \tag{1}$$

$$\alpha = 3V\left(\frac{\varepsilon_p/\varepsilon_m - 1}{\varepsilon_p/\varepsilon_m + 2}\right). \tag{2}$$

where α is the polarizability of the particle. Here V is the particle volume, ε_p is the dielectric function of the particle and ε_m is the dielectric function of surrounding medium. We can see that at a certain wavelength when $\varepsilon_p/\varepsilon_m = -2$ the particle polarizability will become very large. Namely, this is known as the surface plasmon resonance when the scattering cross-section can well exceed the geometrical cross-section of the particle and near-field amplitude of excited electromagnetic wave is much stronger than the incident light wave. Thus, the light trapping can be realized due to local (surface) plasmon excitation (LPE). This is particularly critical in such systems like thin-film solar cells in order to increase light absorption and hence the cell efficiency. For light trapping, it is important that scattering is more efficient than absorption, a condition that is met for larger particles, as follows from Eq. (1). Ag, Al, Au and Cu were found to have much higher so-called optical radiation efficiencies [2] (the energy fraction of the incident light scattered from the particle) than the other metals for a wide range of wavelengths. Strikingly, Ag and Al nanoparticles with diameters around 150 nm were found to exhibit over 90% optical radiation efficiencies for the most actual optical frequencies.

The new term 'plasmonic solar cells' was introduced [3] to characterize such a type of solar cells where light absorption is enhanced by LPE. Depending on the initial conditions, the enhancement factor of 18 times [4], 33%, 19% [5], and 1.7 times [6] could be achieved for the photocurrent using silver nanoparticles on the surface of the device. Reported values for gold nanoparticles are 80% [7], 8% [8], and 3 times [9]. Effect of metallic nanoparticles is not only enhancement of light scattering/absorption but also improvement of the carrier transport [10].

A few main basic mechanisms have been proposed to explain the light absorption (and thus photocurrent) enhancement by metal particles incorporated into or on the solar cells. The first one is discussed above. The second one is based on the prolonged interaction between a semiconductor and light by excitation of a comparably long-living LPE mode (5-10 fs) [7]. The third one could be the electromagnetic field enhancement near the surface of metallic nanoparticles which leads to not only direct absorption enhancement (which is proportional to E^2) but also to the appearance of a non-linear effect in absorbance. The contribution of each mechanism depends on the particle size, the semiconductor absorption and the construction of the solar cell or photodetector.

2. Sample preparation and experimental procedure

Au nanoparticles of 15 nm core size covered by silica shell with ~20 nm thickness were prepared separately [11] as aqua colloid. The geometrical parameters of the prepared NPs were controlled by TEM (Fig. 1). The Au NPs concentration in colloid has been measured just before deposition from spectral dependence of extinction (Fig. 2). It was about 2.0×10^{18} m^{-3}. The NPs were diluted 30 times in acetone and placed electrophoretically (Fig. 3) onto GaAs surface with backside Ohmic contacts. The NPs in aqua/acetone mixture are charged negatively by adsorbed hydroxile groups (–OH). Therefore, to move and deposit the NPs on GaAs substrate it should be connected to positive electrode of the electrophoretic cell. This can potentially cause substrate etching. That is why it is important to apply the lowest possible potential to the cell to avoid substrate corrosion. An additional set of experiments was done to determine potential (2 V) and time (1 hour) for the NPs deposition when substrate corrosion was not observed, which was confirmed by AFM measurements.

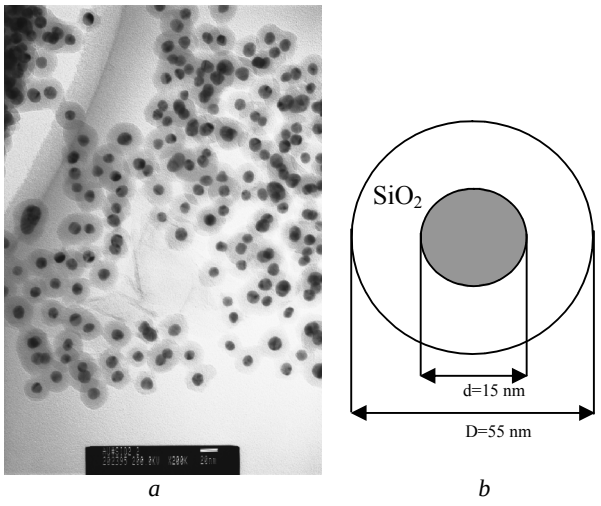

Fig. 1. a) TEM image of the core-shell structure of Au NPs used in experiments. b) Particle sizes.

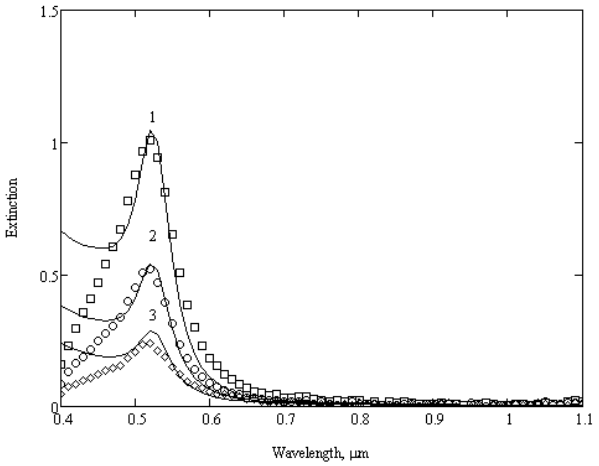

Fig. 2. Experimental (points) spectral dependences of extinction (log(1/*T*)) for various concentrations of Au NPs in solution 100% (*1*), 50% (*2*) and 25% (*3*). Solid lines are calculation results using the Mie theory for NPs with the original concentration 2.022×10^{18} m^{-3} and size shown in Fig. 1b.

All AFM measurements were carried out using a NanoScope TM IIIA controller and a Dimension TM 5000 stage. The Si_3N_4 tip had radius of about 10 nm. Images were captured in the tapping mode on 3 × 3μm scan area. The AFM image of the prepared samples shows (Fig. 4) densely packed film of the NPs with a number of particles about 10^{10} cm^{-2}.

The average thickness of the deposited NPs-based films was obtained from the measurements of reflectance in the wavelength range 0.4-1.1 μm at different angles of polarized light incidence. The measuring setup includes a tungsten lamp light source, light chopper, monochromator, polarizer of the Glan prism type, photodetector with an amplifier, rotating sample holder, and controller computer. Additional calculations show that the highest sensitivity to the thickness of thin film containing Au can be obtained from the relative reflectance at the angle of light incidence about 60 degs. Therefore, the reflectance measurements were carried out at this angle and the results were normalized on the reflectance of free GaAs substrate.

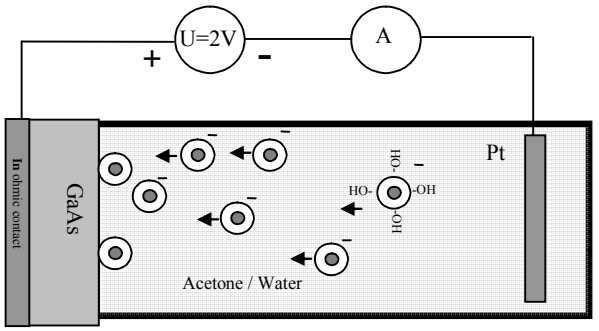

Fig. 3. Simplified sketch of the cell for Au NPs deposition.

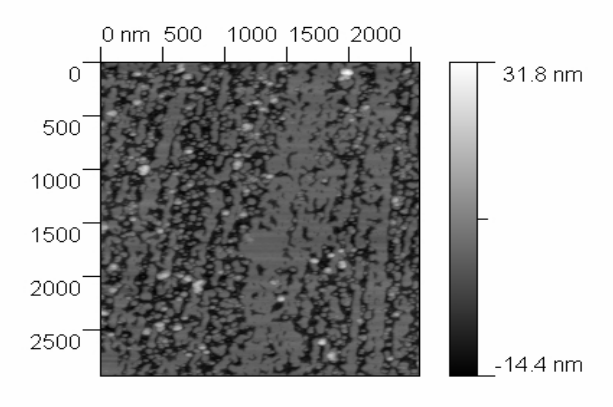

Fig. 4. AFM image of GaAs surface with Au nanoparticles deposited electrophoretically.

After the NPs deposition, two types of the surface barrier structures were formed by evaporation of thick continuous (61 nm) Au solar cell type contacts and thin (23 nm) semitransparent Au circular contacts with the diameter 1.3 mm in a vacuum chamber at the residual pressure of 10^{-5} Torr (Fig. 5). Such contact types were chosen to discriminate the effects connected with local plasmon excitation from those connected with the Au film transparency.

The measurements of photocurrent were done on the same setup used for the reflectance measurements except of the additional lock-in amplifier for the weak signal from the prepared surface barrier structures.

The NPs film thickness obtained from reflectance measurements (Fig. 6) was 55 nm and coincides with the NPs diameter. It means that the monolayer of the NPs was deposited on GaAs surface.

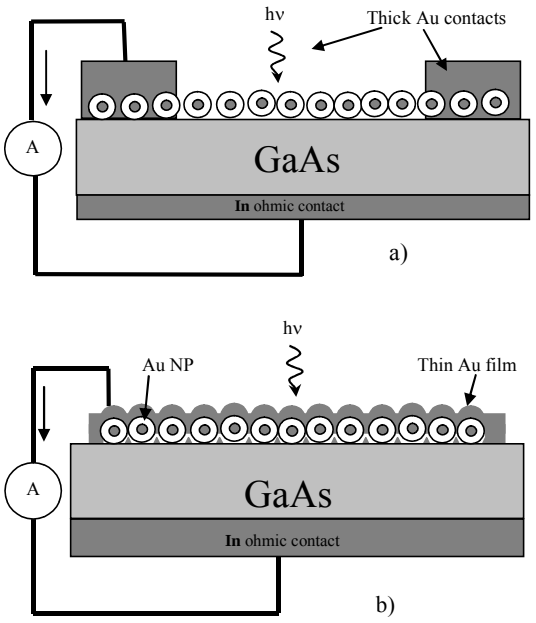

Fig. 5. The structures under the study: with thick 61 nm (a) and thin 23 nm semitransparent (b) Au contacts.

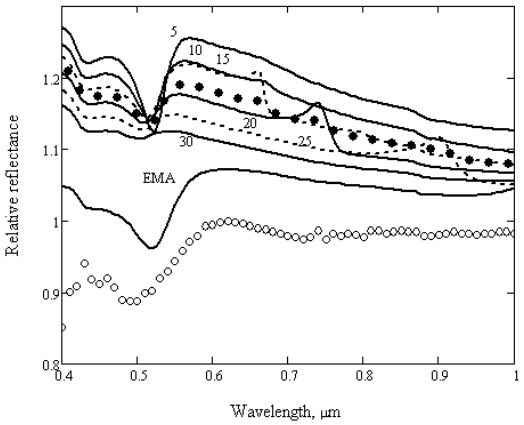

Fig. 6. Experimental (open dots) and calculated ratio of reflectance spectra of GaAs with Au NPs to reflectance spectra of GaAs without them. Filled dots are curve that is calculated as average between curves with numbers. The measurement was done under *p*-polarized light with 60º angle of light incidence. The numbers near the curves on the figure are the distances between NP. Parameters for calculations: outer NP diameter is 55 nm, Au core diameter is 15 nm, shell is SiO_2 with the refractive index $n = 1.47$. NPs placed in triangular cell on GaAs substrate. The curve pointed as EMA shows the calculation result using the simple effective medium approximation theory with parameters: film thickness is 55 nm, Au volume fraction is $f = 0.0071$.

3. Results and discussion

The measurement of extinction (Fig. 2) gives the position of local plasmon resonance which is around 0.52 μm for this type of particles. Au NPs have a thick shell (about 20 nm) made of silica with the refractive index about $n = 1.47$. Therefore, we can expect that the local plasmon resonance position will not be changed after the NPs deposition on GaAs substrate as compared to that of Au NPs colloids in water, and finally we have to search the contribution into the photocurrent at the wavelength close to 0.52 μm.

The relative reflectance spectrum (Fig. 6) shows minima at 0.52 μm wavelengths. They appeared due to absorption in Au NPs. First we tried to describe the reflectance by a simple optical model of the effective film of Au NPs with a thickness h on GaAs substrate. The dielectric permittivity of this film ε_{eff} can be approximated using Bruggeman's effective medium theory (EMA) [12]:

$$f\frac{\varepsilon_{\text{eff}}-\varepsilon_{\text{Au}}}{\varepsilon_{\text{Au}}+2\varepsilon_{\text{eff}}}+(1-f)\frac{\varepsilon_{\text{eff}}-\varepsilon_{d}}{\varepsilon_{d}+2\varepsilon_{\text{eff}}}=0, \qquad (3)$$

where f is the volume fraction of Au in the film, ε_{Au} and ε_d are dielectric permittivities of Au and silica+voids mixture, respectively. The best fit was obtained for $h = 55$ nm and $f = 0.0071$. The obtained effective film thickness coincides with the diameter of nanoparticles. This is one more evidence of the deposition of only the single layer of nanoparticles.

Few words have to be said about the choice of 60 degrees angle of light incidence and relative reflectance. An additional set of calculations (not shown here) for thin (few nanometers) Au films placed on GaAs showed that the most intensive minima (at 0.5 μm) related to Au film appeared at 60 degrees angle of incidence. Therefore, measurements at this angle of incidence are the most sensitive to presence of Au NPs on GaAs surface. It has to be mentioned that some features appear in reflectance spectra of GaAs substrate and GaAs+Au NPs due to peculiarities in optical constants of GaAs itself at 0.45 μm wavelength. Therefore, to exclude them from analysis we used relative spectra, namely, the ratio of reflectance of GaAs+Au NPs to reflectance of a free GaAs substrate.

The minimum around 0.52 μm was caused by interband transitions of gold itself as well as by local plasmon excitation. Because of quite small Au core size, the effect of local plasmon excitation on reflectance decrease is expected to be small at this wavelength as compared to the effect of interband transitions. Therefore, the application of effective medium approximation to describe such an effective film is reasonable and gives the correct results.

This rough description of light interaction with a layer of NPs on the surface using EMA cannot give the whole picture obviously, therefore we tried to apply exact formalism to calculate the light transmittance into GaAs substrate. These theoretical calculations of light propagation through ensemble of Au NPs in regime of surface polaritons and local modes excitation are based on the curvilinear coordinates transformation method in the differential formalism framework for the system of Maxwell's equations [13]. In this method, the boundary conditions are simplified to the continuity of in-plane covariant components of electromagnetic field by the introduction of a curvilinear non-orthogonal coordinates system at each non-flat interface.

By analogy with the calculations of light propagation trough 1D cylindrical nanowire ensemble system [14], the 2D periodic ensemble of the plasmon-carrying (metal) spherical nanoparticles with a dielectric shells is considered as a three-layer system "dielectric/metal/dielectric" surrounded by air with closing up non-flat profiles (Fig. 7). These profiles confine the symmetric films [15] and are defined by the periodic functions, $\xi(x,y)$, with periods l_x and l_y , and one can be written for one elementary cell in the form

$$\xi(x,y) = -\frac{d_{\text{eff}}}{2} + \begin{cases} \sqrt{a^2 - x^2 - y^2}, & \sqrt{x^2+y^2} < a \\ 0, & \sqrt{x^2+y^2} \geq a \end{cases}, \quad (4)$$

where x and y are the Cartesian coordinates ($|x| \leq l_x/2$ and $|y| \leq l_y/2$), a is the sphere radius for cores or shells, and d_{eff} is the flat film thickness with an equivalent volume of nanoparticles array with or without shells.

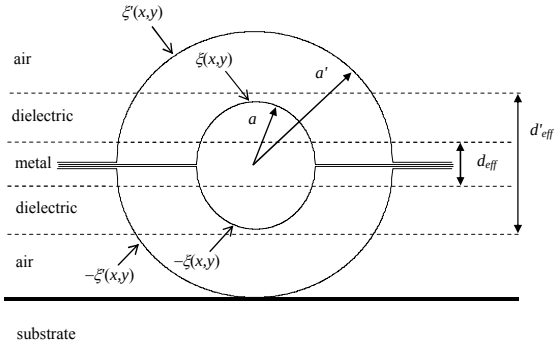

Fig. 7. Schematic cross-section of single metal nanoparticle covered by dielectric shell on flat substrate.

The results of calculation of relative reflectance are shown in Fig. 6 for different distances between the NPs surfaces that are placed into the triangular cell. Experimental (open dots) and calculated ratios of reflectance spectra show few peculiarities with different behavior depending on the distance between NPs. First of all, the feature at 0.52 μm is independent on the distance between NPs. Therefore, we associate it with LPE. Few peculiarities appearing for the different distances between NPs (15, 20, 25 nm) as oscillations at different wavelengths can be related to the surface plasmon polariton (wave) excitation (SPP) because of the periodicity in the considered system and its behavior that depends on the period (distance between NPs surfaces). The resonance wavelength increases as the period increases, which is in agreement with SPP behavior. In practice, for real prepared samples the periodicity in location of NPs is low (AFM image in Fig. 4), and thus only a short-range order exists. Therefore, the excitation of SPP is hardly to be expected. And we have to average the curves with different distances (curve marked by filled dots in Fig. 6) for comparison with the experiment. As it was expected, the features connected to SPP were disappeared while for LPE it remained at 0.52 μm which is seen from experiment and by calculations.

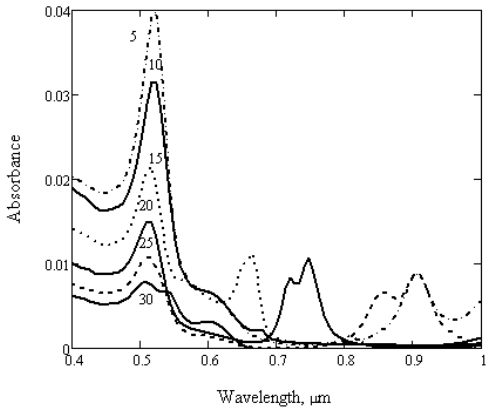

Fig. 8. Calculated absorbance spectra of Au NPs placed on GaAs in triangular cell with the distance between NPs (in nm) shown in the figure. Parameters for calculations: outer NP diameter is 55 nm, Au core diameter is 15 nm, shell is SiO_2 with the refractive index n = 1.47.

The absorbance calculated separately (Fig. 8) allows to identify the excitation of any modes in the system, because any of them increases the energy dissipation in metallic particles. Indeed, we observe the mode at 0.52 μm which is independent of the interparticle distance and therefore related to LPE. Few modes at various wavelengths depend on interparticle distance and, as told above, are related to SPP.

After reflectance analyses where LPE was observed, we tried to ascertain their contribution into the photocurrent of the GaAs based surface barrier structures. Two types of samples have been prepared. The first one was made with thick (61 nm) Au solar cell type barrier contacts. These contacts have a low transmittance and the total photocurrent is caused only by a part of surface on the distance of minor carriers (holes in our case) diffusion length (few microns) from contact edges. Therefore, the absolute value of photocurrent is quite small, but this type of samples is best in correspondence to the theoretical calculation model. The second type was made by deposition of thin (23 nm) Au film through the mask with circular dots (1.3 mm diameter) onto the GaAs substrate

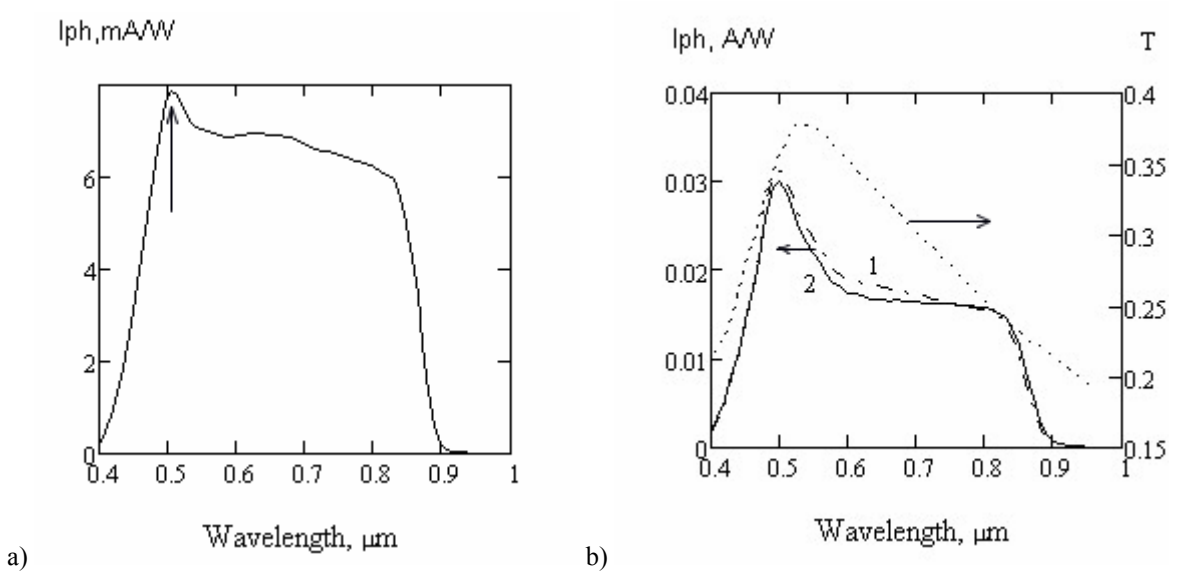

a) b)

Fig. 9. Spectral dependences of the photocurrent on wavelength for Au/GaAs structures with thick (a) and thin (b) Au contacts. Curve 1 in the figure b is for structure with Au NPs and curve 2 without them, dotted curve is transmittance of the light into the GaAs substrate through the continuous film of Au with 21 nm thickness.

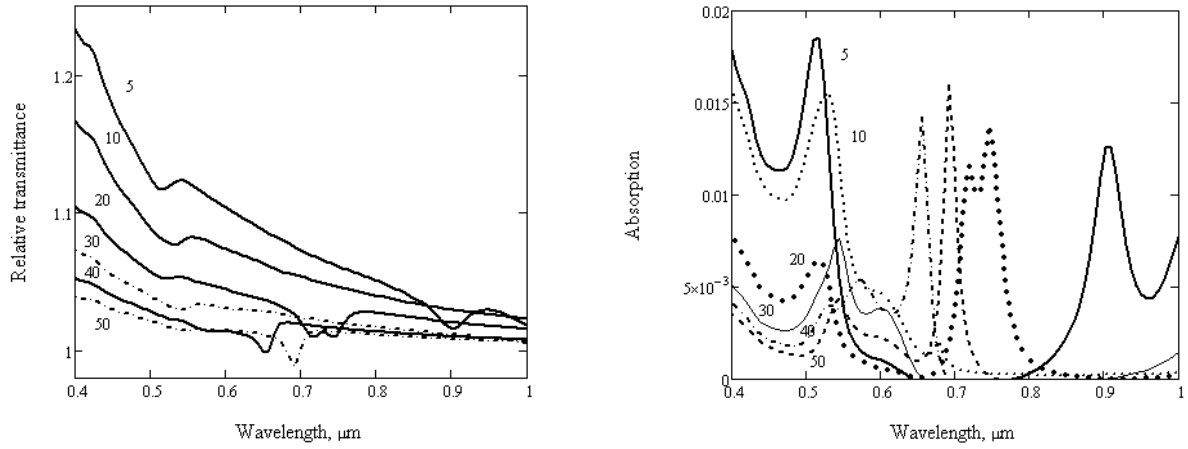

a) b)

Fig. 10. a) Calculated transmittance spectra of the light into the GaAs substrate with Au NPs on the top. The angle of light incidence is 0º. The numbers in the figure are the distance between NP in nm. Parameters for calculations: outer NP diameter is 55 nm, Au core diameter is 15 nm, shell is SiO_2 with the refractive index $n = 1.47$. NPs are placed in triangular cell on GaAs substrate. b) Corresponding Au NPs absorption spectra.

with deposited NPs. The active region generating the photocurrent is larger in this case, but the total spectrum is modulated by the transmittance spectrum of thin Au film. Fig. 9 shows that both types of samples exhibit the peak in photocurrent at 0.52 μm wavelength. In the case of thick Au contacts, the peak is caused by light transmittance through Au NPs with LPE contribution due to generation of photocarriers directly by evanescent electromagnetic waves. The peak for samples with thin barrier contacts (Fig. 9b) is mostly pronounced, because of the transmittance peak of Au film practically coincides with LPE peak. Therefore, it is hard to distinguish the contribution of LPE from the transmittance of Au film. But in this case, the structures with Au NPs show larger photocurrent (Fig. 9b, curve 1) as compared to the similar structures without them (curve 2). And we associate this with the contribution of LPE.

The light transmittance into GaAs substrate through the Au NPs monolayer film was calculated theoretically at normal incidence using the same formalism (Fig. 10). The transmittance spectrum (Fig. 10a) also shows few minima corresponding to LPE and SPP that are conformed by analogous absorbance spectra (Fig. 10b). And as was discussed earlier, experimentally we observe only LPE contribution due to averaging effect. One could ask, why the photocurrent has its maximum at the wavelength of LPE, while the transmittance spectrum has its minimum there? The answer could be in photocurrent generation mechanism that is not the direct generation of photocarriers by transmitted light but generation by evanescent enhanced electromagnetic field as well as by scattered and reradiated local plasmons. An additional component could be the non-uniform planar distribution of the electromagnetic filed along the surface of semiconductor, which leads to the additional component in derivatives of the electromagnetic wave flow to which the carrier generation function is proportional.

4. Conclusions

The method for theoretical calculation of the interaction between light and the surface barrier structures with deposited Au NPs has been proposed. Local plasmons make notable contribution into the photocurrent and can be used for the photocurrent enhancement in solar cells and photodetectors. The value of contribution can be increased by optimization of Au NPs size and sample construction.

References

1. C.F. Bohren, D.R. Huffman, *Absorption and Scattering of Light by Small Particles*. Wiley Interscience, New York, 1998.
2. K. Tanabe, Optical radiation efficiencies of metal nanoparticles for optoelectronic applications // *Materials Letters* **61** (23-24), p. 4573-4575 (2007).
3. K.R. Catchpole, A. Polman, Plasmonic solar cells // *Opt. Express* **16** (26), p. 21793-21800 (2008).
4. H.R. Stuart, D.G. Hall, Island size effects in nanoparticle-enhanced photodetectors // *Appl. Phys. Lett.* **73** (26), p. 3815-3817 (1998).
5. S. Pillai, K.R. Catchpole, T. Trupke, M.A. Green, Surface plasmon enhanced silicon solar cells // *J. Appl. Phys.* **101**, 093105-093113 (2007).
6. J. He, P. Yang, H. Sato, Y. Umemura, A. Yamagishi, Effects of Ag-photodeposition on photocurrent of an ITO electrode modified by a hybrid film of TiO_2 nanosheets // *J. Electroanalyt. Chem.* **566** (1), p. 227-233 (2004).
7. D.M. Schaadt, B. Feng, E.T. Yu, Enhanced semiconductor optical absorption via surface plasmon excitation in metal nanoparticles // *Appl. Phys. Lett.* **86** (6), p. 1-3 (2005).
8. S.H. Lim, W. Mar, P. Matheu, D. Derkacs, E.T. Yu, Photocurrent spectroscopy of optical absorption enhancement in silicon photodiodes via scattering from surface plasmon polaritons in gold nanoparticles // *J. Appl. Phys.* **101** (10), 104309 (2007).
9. N. Chandrasekharan, P.Y. Kainat, Improving the photoelectrochemical performance of nanostructured TiO_2 films by adsorption of gold nanoparticles // *J. Phys. Chem. B* **104** (46), p. 10851-10857 (2000).
10. T. Lana-Villarreal, R. Gomez, Interfacial electron transfer at TiO_2 nanostructured electrodes modified with capped gold nanoparticles: The photoelectrochemistry of water oxidation // *Electrochem. Communs* **7** (12), p. 1218-1224 (2005).
11. Y.S. Park, L.M. Liz-Marzan, A. Kasuya, Y. Kobayashi, D. Nagao, M. Konno, S. Mamykin, A. Dmytruk, M. Takeda, N. Ohuchi, X-ray absorption of gold nanoparticles with thin silica shell // *J. Nanoscience and Nanotechnology* **6**, p. 3503-3506 (2006).
12. D.A.G. Bruggeman, Berechnung verschiedener physikalischer Konstanten von heterogenen Substanzen. I. Dielektrizits konstanten und Leitfhigkeiten der Mischkrper aus isotropen Substanzen // *Annalen der Physik* **416** (7), S. 636-664 (1935).
13. A.V. Korovin, Improved method for computing of light-matter interaction in a multilayer corrugated structures // *JOSA A* **25**, p. 394-399 (2008).
14. N. Dmitruk, T. Barlas, A. Dmytruk, A. Korovin, V. Romanyuk, Synthesis of 1D regular arrays of gold nanoparticles and modeling of their optical properties // *J. Nanoscience and Nanotechnology* **8**, p. 564-571 (2008).
15. N.L. Dmitruk, A.V. Korovin, High light transmission through thin absorptive corrugated films // *Opt. Lett.* **33**, p. 893-895 (2008).